This article was downloaded by:
On: *25 January 2011*
Access details: *Access Details: Free Access*
Publisher *Taylor & Francis*
Informa Ltd Registered in England and Wales Registered Number: 1072954 Registered office: Mortimer House, 37-41 Mortimer Street, London W1T 3JH, UK

Liquid Crystals
Publication details, including instructions for authors and subscription information:
http://www.informaworld.com/smpp/title~content=t713926090

Phases, phase transitions and confinement effects in a series of antiferroelectric liquid crystals

Jan P. F. Lagerwall; Deven D. Parghi; Daniel Krüerke; Fathi Gouda; Pontus Jägemalm

Online publication date: 11 November 2010

To cite this Article Lagerwall, Jan P. F. , Parghi, Deven D. , Krüerke, Daniel , Gouda, Fathi and Jägemalm, Pontus(2002) 'Phases, phase transitions and confinement effects in a series of antiferroelectric liquid crystals', Liquid Crystals, 29: 2, 163 — 178
To link to this Article: DOI: 10.1080/02678290110092634
URL: http://dx.doi.org/10.1080/02678290110092634

PLEASE SCROLL DOWN FOR ARTICLE

Full terms and conditions of use: http://www.informaworld.com/terms-and-conditions-of-access.pdf

This article may be used for research, teaching and private study purposes. Any substantial or systematic reproduction, re-distribution, re-selling, loan or sub-licensing, systematic supply or distribution in any form to anyone is expressly forbidden.

The publisher does not give any warranty express or implied or make any representation that the contents will be complete or accurate or up to date. The accuracy of any instructions, formulae and drug doses should be independently verified with primary sources. The publisher shall not be liable for any loss, actions, claims, proceedings, demand or costs or damages whatsoever or howsoever caused arising directly or indirectly in connection with or arising out of the use of this material.

LIQUID CRYSTALS, 2002, VOL. 29, NO. 2, 163–178

Taylor & Francis
Taylor & Francis Group

Phases, phase transitions and confinement effects in a series of antiferroelectric liquid crystals

JAN P. F. LAGERWALL*, DEVEN D. PARGHI†, DANIEL KRÜERKE†, FATHI GOUDA‡ and PONTUS JÄGEMALM

Chalmers University of Technology Dept. for Microelectronics and Nanoscience; Liquid Crystal Physics SE-412 96 Göteborg, Sweden
†Technische Universität Berlin Iwan N. Stranski Institut Str. des 17 juni 112, 10623 Berlin, Germany
‡Umm-Al Qura University Physics Department, P.O. Box 6427, Makkah, Saudi Arabia

(*Received 21 May 2001; in final form 3 August 2001; accepted 13 August 2001*)

Using a variety of optical and electro-optical techniques, as well as dielectric spectroscopy, we have investigated three homologues in the chiral liquid crystal series *n*F1M7, where *n* denotes the length of the unbranched terminal chain. The main focus of the study is the series of smectic C subphases, i.e. SmC^*_α, $SmC^*_{1/3}$ and $SmC^*_{1/4}$. During switching in the SmC^*_α phase, a peculiar redirection of the plane of biaxiality, distinguishing this phase from SmA* and SmC*, was observed. We present a simple explanation for this behaviour which correlates well with the clock model description of the SmC^*_α phase. We found a zero mesoscopic polarization for the $SmC^*_{1/4}$ phase and a non-zero mesoscopic polarization for $SmC^*_{1/3}$, observations which are consistent with a distorted clock model. The dielectric spectroscopy investigations, performed at several different cell gaps, clearly show that the dielectric response in these materials is easily dominated by surface-induced structures if the cell gap is reduced, thus reflecting that the bulk thermodynamic phase exists in very thick cells only.

Downloaded At: 17:51 25 January 2011

1. Introduction

Since the recognition of anticlinic order in smectic liquid crystals [1], an intriguing problem for liquid crystal scientists has been to understand what variants of the chiral smectic C phase are possible and to elucidate their structures. In particular, it has proved to be difficult to obtain a coherent picture of the two phases often found between SmC* and SmC^*_A, as well as to disclose the nature of the SmC^*_α phase [2–4]. These three phases are often collectively called the chiral smectic C subphases. Two main theoretical models have been proposed: the Ising model [5] and the clock model [6], neither of which agrees with all the experimental evidence. Recently, it has been proposed that the most realistic description of the subphases may be found using a distorted clock structure [3, 7, 8].

Not only is the understanding of the subphases an important issue from a fundamental point of view, but it has also been shown that the applicationally important SmC* and SmC^*_A phases may behave quite differently depending on which other phases are present in the phase sequence [9–12]. Furthermore, during the last few years it has become clear that the experimental conditions under which the materials are studied may affect the phase behaviour to an extent previously not commonly recognized [13–15]. In particular, a strong surface influence may produce not only geometries different from those of the bulk phases, but also large shifts in phase transition temperatures, phase coexistence and in some cases even complete expulsion of phases [16–20].

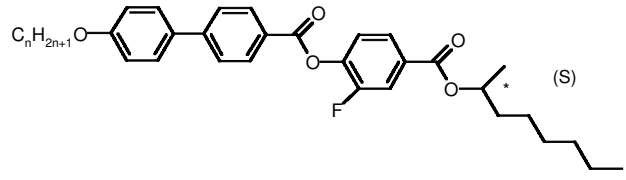

Figure 1. Chemical structure of the investigated homologous series (*S*)-*n*F1M7.

In this work we have studied three homologues in a series of antiferroelectric liquid crystal materials, denoted (*S*)-*n*F1M7 (cf. figure 1 and the table), together representing all well-established† phases within the chiral

*Author for correspondence; e-mail: jpf@fy.chalmers.se

†Here we mean phases thermodynamically stable in bulk samples in the absence of electric and magnetic fields.

Liquid Crystals ISSN 0267-8292 print/ISSN 1366-5855 online © 2002 Taylor & Francis Ltd
http://www.tandf.co.uk/journals
DOI: 10.1080/02678290110092634

Table. Phase sequences on heating the homologues *n*F1M7, as obtained by dielectric spectroscopy measurements in thick (≈ 40 μm) cells. Other techniques may give slightly different transition temperatures. Earlier reports on 12F1M7 [16, 21–23] and 11F1M7 [24] present slightly different phase sequences for these compounds as the authors interpret the response between $SmC^*_{1/4}$ and SmA* differently from us (see § 3.2.1). On cooling, supercooling effects are important and may explain the slightly lower transition temperatures reported in, for instance, [15]. The saturated $\mathbf{P}_s$ and tilt angle values are approximations 65°C below the transition between SmA* and SmC*/SmC^*_α [25].

n	Phase sequence on heating (transition temperatures in °C)	Saturated $\mathbf{P}_s$/nC m^{-2}	Saturated tilt/degrees
10	SmC^*_A–76.5–$SmC^*_{1/3}$–78.5–$SmC^*_{1/4}$–81.5–SmC^*_α–84–SmA*	95	25
11	SmC^*_A–70–$SmC^*_{1/3}$–76–$SmC^*_{1/4}$–80.5–SmC*–89–SmA*	105	27
12	SmC^*_A–79.5–$SmC^*_{1/3}$–83–$SmC^*_{1/4}$–85–SmC*–92–SmA*	100	27

smectic C family. Experimental data from a variety of investigative techniques, using several different sample geometries, have been compared in order to distinguish better those features which are truly characteristic of the different phases from those that may be artefacts originating from, for example, phase coexistence or surface-induced structures. The results obtained can be understood using the distorted clock model, even though they by no means prove it to be correct.

Among the three compounds studied in the present work, one, 12F1M7, has already been extensively studied and described in the literature [21–23], often under the code name AS-573‡. We include it in our study mainly for completeness, enabling a comparison of our results with those of previous work. Reports on the two other homologues are much scarcer, despite the fact that in many respects they can be regarded as more interesting. For instance, the 11F1M7 compound, to our knowledge previously reported in only one publication by Panarin *et al.* [24], has unusually large temperature ranges of the subphases between SmC* and SmC^*_A. In the third compound, on which we have been unable to find any reports in previous literature, the SmC* phase is replaced by SmC^*_α. As will become clear below, this difference has a drastic effect on the general phase behaviour; in particular the response to increased surface influence is completely different from that of the two homologues exhibiting the SmC* phase.

Many different names and abbreviations have been proposed for the subphases between SmC* and SmC^*_A, but some of these suggest properties which are not necessarily present (e.g. ferrielectricity) [26]. What seems to be clear, however, is that the size of the unit cell, i.e. the number of layers comprising the repeated structure, is four for the high temperature phase and three for the other one. Both the Ising model and the clock model predict these numbers and they have also recently been confirmed experimentally for a limited number of compounds [4]. In this paper we follow the convention proposed by Lagerwall [15] and use the corresponding wave number to denote the phases, thus referring to them as $SmC^*_{1/3}$ (often called SmC^*_γ) and $SmC^*_{1/4}$ (sometimes referred to simply as 'AF').

‡In this paper we use the denomination *n*F1M7 as initially proposed by Nishiyama *et al.* [26].

2. Experimental

Conoscopic switching studies and optical spectroscopy measurements were performed on thick free-standing films (≈ 5000 smectic layers), which we regard as a good approximation to bulk samples. The films were prepared by spreading the compound over a slit-like opening in a printed board. The board is equipped with copper electrodes permitting an electric field to be applied across the film in the plane of the smectic layers. The width of the slit in the direction of the applied field was 1 mm for conoscopy studies and 3 mm for the spectrophotometer experiments. During the conoscopic investigations, the electric field was generated by a Leader LFG-1300 frequency generator (adjusted frequency 1–2 Hz) and amplified by a high voltage amplifier (Kepco BOP 1000M). For temperature control, the film holder was placed on an open Linkam heating stage. The film was observed in transmission using a Leica ortholux-II-pol microscope equipped with either linear or circular polarizers, a monochromator, and a special microlens adapted for conoscopy (Nicon Mplan x40 0.5 ELDW 210/0). For measuring the optical transmittance as a function of wavelength, a Shimadzu 3101PC spectrophotometer (190–3200 nm measuring range) was used and the sample was inserted such that the light beam entered the film at normal incidence, i.e. parallel to the smectic layer normal. The film thickness was estimated from the interference pattern observed in the spectrum. The sample temperature was controlled using a Julabo FP4 temperature regulator (±0.1°C stability). The transmittance was measured both on cooling and on heating for all three compounds.

Dielectric spectroscopy studies were performed using an HP 4192 dielectric bridge (5 Hz–13 MHz measuring range). The sample temperature was regulated using a Julabo F25-HD temperature controller with a custom-made liquid-heated hot stage (better than ±0.1°C stability).

Downloaded At: 17:51 25 January 2011

All measurements were performed both on heating and on cooling, and three different values of the measuring field (5, 12.5 and 20 mV μm^{-1}) were used in order to verify that no artefacts due to an inappropriate measuring field were introduced. The spectra presented here were taken with 12.5 mV μm^{-1} measuring field strength, and no d.c. bias was applied during the course of the measurements.

In order to obtain a good picture of how the cell surfaces influence the liquid crystal, we developed a special type of wedge-shaped sample cell for dielectric spectroscopy, permitting measurements at varying cell gap; figure 2 shows the construction of this cell. One substrate carries a 4 mm wide electrode along the whole length of the cell, while there are seven narrow (0.2–0.5 mm wide) transverse electrodes, placed at different distances from one narrow end of the cell, on the other substrate. Prior to gluing the substrates together, a 50 μm mylar spacer is placed close to one narrow end of the cell. By repeating the same measurement procedure with different transverse electrodes connected to the equipment, we were able to assess the influence of a decreasing cell gap on the dielectric response, without moving the sample or even opening the hot stage. Moreover, as one single cell was used for all measurements, there were no variations in alignment layers and cell preparation.

The electro-optic studies were performed on the 10- and 12 F1M7 homologues only, on cooling from the SmA* phase. Transmission vs. voltage curves, taken at 0.1, 1 and 10 Hz switching frequencies, were recorded on a Gould 1624 oscilloscope using an SMT photomultiplier attached to a WILD M420 microscope. The applied fields were generated by a Kiethley 3930A multifunction synthesizer connected to a Krohn-Hite 7500 power amplifier. The samples (1.4, 4 and 10 μm cell gap) were aligned by applying a square-wave a.c. field (100 Hz) on slow cooling from the isotropic phase into SmA*.

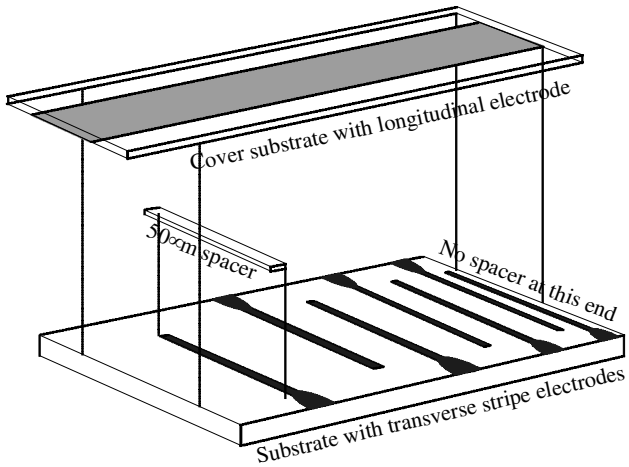

Figure 2. Construction of the wedge-shaped measurement cell.

All cell substrates were coated with polyimide to ensure a planar alignment of the liquid crystal. Both substrates of the cell type used for electro-optic measurements were buffed in the same direction, while the wedge cells used for dielectric spectroscopy had one buffed and one unbuffed substrate.

The polarization and tilt angle as a function of temperature have been measured previously [25] and selected values are given in the table.

3. Results and discussion

3.1. *Free-standing films*

3.1.1. *Conoscopy*

Conoscopic images provide information about the shape and orientation of the macroscopic optical indicatrix, which in smectic phases is related to both the molecular polarizability and the arrangement of the molecules within and across the layers. Distortions induced by electric fields (e.g. helix unwinding, variations of tilt angle, or changes in the unit cell composition) result in transformations of the initial conoscopic image into one that is characteristic of the distorted phase architecture [27]. Displacements of the entire image correspond to tilting of the indicatrix, while a splitting of the isogyres (the cross turning into two hyperbolae) corresponds to a transformation from a uniaxial to a biaxial structure. In the tilted phases, which in the chiral compounds studied here possess a helical macrostructure, the response can be quite complex. Conoscopy studies have been performed on the $n = 12$ homologue by Panarin *et al.* [15] and Baylis *et al.* [21], but no previous work of this type on 11- or 10 F1M7 is known to us.

Very interesting is the conoscopic behaviour of the SmC^*_α phase which, according to the clock model [6], should be characterized by a small tilt and extremely short pitch (5–10 layers), incommensurate to the layer spacing. On applying an electric field over such a structure, we may expect to see two kinds of response. First the electroclinic effect (field-induced change of the tilt angle, θ) will shift the conoscopic image perpendicular to the field direction, reflecting the tilting of the macroscopic indicatrix. However, as this is now a helical structure, the electroclinic effect will induce an observable macroscopic biaxiality, i.e. a splitting of the isogyres, distinctly different from the SmA* case. Provided that the helix unwinding is small enough to be neglected, a reasonable assumption for low field strengths in this phase, the electroclinic effect will lead to a larger tilt angle in layers where the polarization initially has a component along the applied electric field, and a smaller tilt angle in all other layers. This will lead to an isogyre splitting directed *along* the electric field, so the result will be an image 'stretched' in the field direction, but shifted in a

Downloaded At: 17:51 25 January 2011

direction perpendicular to it. Such an image was indeed observed at intermediate field strengths (below 1 V μm^{-1}) in the SmC^*_α phase of 10F1M7 (figure 3, upper row). On increasing the field to 1 V μm^{-1}, unwinding of the helix was achieved and the isogyres split *perpendicularly* to the field.

Exactly the same behaviour should in principle be seen in the SmC* phase, but here the helix starts to unwind even at rather low field strength, resulting in a large macroscopic biaxiality parallel to the tilting direction, seen as an isogyre splitting perpendicular to the applied field. In addition, as soon as the equilibrium tilt angle becomes comparatively large (even some degrees below the SmA*–SmC* transition) the contribution from the electroclinic effect becomes negligible, so the expected SmC* conoscopic response is what was observed for 11- and 12 F1M7 in this phase (figure 3, lower row).

Both Baylis *et al.* and Panarin *et al.* reported a changing behaviour on cooling throughout the SmC* phase of 12F1M7. Based on their observations, neither of which we could reproduce either on 11- or on 12 F1M7, they propose that this temperature region in fact exhibits more than one phase. Panarin *et al.* noticed a blurry image on the way to switching the sample to the unwound synclinic state at low temperatures of the SmC* phase. While the behaviour of the SmC* phase in our study was perfectly normal, we did observe such a blurry state during switching within the $SmC^*_{1/4}$ phase, the phase which bounds the SmC* phase on the low temperature side. As described below, the $SmC^*_{1/4}$ phase exhibits a field-induced intermediate state producing a conoscopic image reminiscent of that of the unwound $SmC^*_{1/3}$ phase. While switching from the simple unwound $SmC^*_{1/4}$ state (figure 4, upper row, ± 700 V pictures) to the intermediate state (same figure and row, ± 1000 V pictures), a blurry image similar to that described by Panarin *et al.* was observed. Most certainly, this is a superposition of the two images formed at ± 700 and ± 1000 V, respectively, arising from the fact that the transition from one state to the other does not take place instantaneously throughout the sample. Baylis *et al.* do not describe the blurry image during switching, but in the same temperature region they experienced a discrete jump from one low tilt state to the opposite, with the helix rewinding only if the switched field was turned off.

A possible explanation for the differences between our study and those mentioned above is that we performed the measurements on free-standing films while both earlier studies were carried out using cells prepared with a homeotropic alignment agent. In particular, in the case of the Baylis *et al.* study, where the cell cannot be considered very thick (23 μm), one can contemplate the presence of surface pinning effects, which may slow the helix rewinding such that it does not occur during a.c. switching. This hypothesis is strengthened by the fact that they observed the full-pitch SmC* selective reflection band, showing that the helix must have been tilted in their sample [28]. Hence, the alignment layer must induce quite a strong director anchoring at the surface, restricting the tilt angle with respect to the surface such that the whole layer structure tilts. With increasing tilt angle on cooling through SmC*, it is not unreasonable that the reformation of the helix after unwinding becomes increasingly hindered by such a surface anchoring. We observed the same inclined helix in homeotropic cells (not further discussed in this work due to the undesired geometry), while the free-standing films showed

Downloaded At: 17:51 25 January 2011

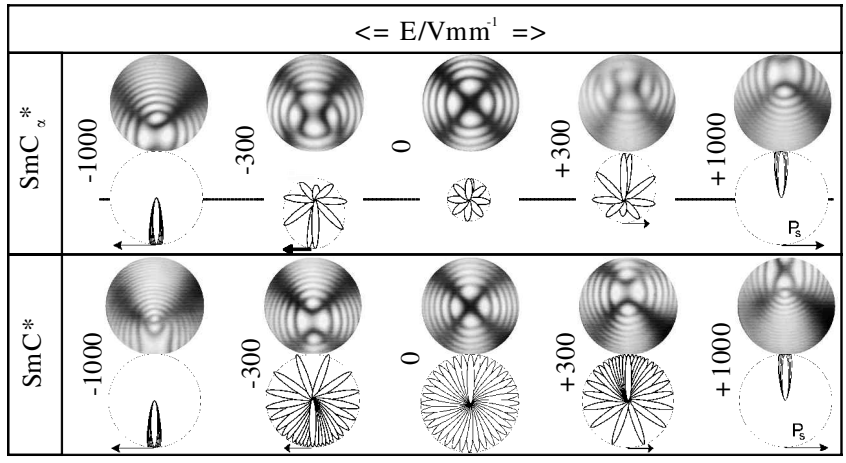

Figure 3. Switching behaviour as observed by conoscopy in the SmC* phase of 11F1M7 and the SmC^*_α phase of 10F1M7. The micrographs are obtained using monochromatic light with a wavelength $\lambda = 435$ nm. Below the conoscopic images possible corresponding director structures based on the distorted clock model are sketched. The electric field is directed horizontally.

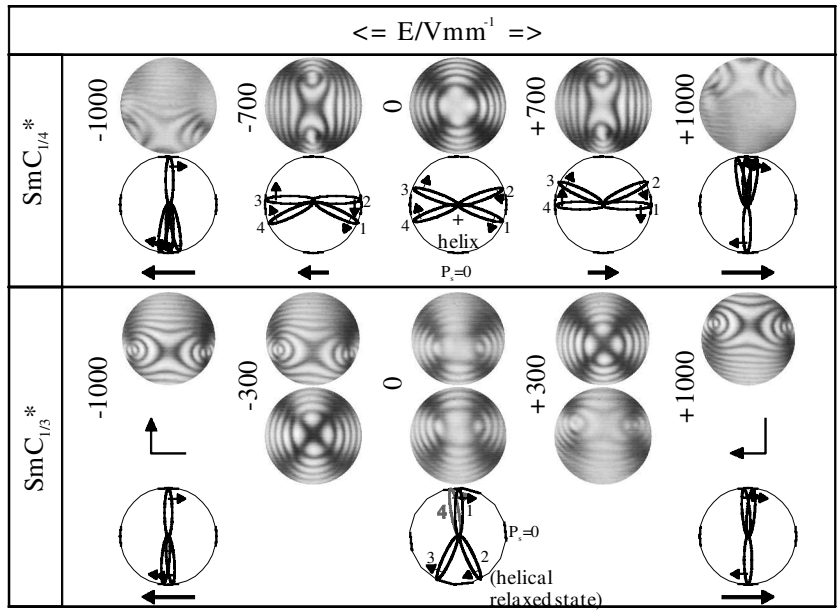

Figure 4. Switching behaviour as observed through conoscopy in the $SmC^*_{1/4}$ phase of 11F1M7 and the $SmC^*_{1/3}$ phase of 10F1M7. The micrographs are obtained using monochromatic light with a wavelength $\lambda = 435$ nm. Below the conoscopic images possible corresponding director structures, based on the distorted clock model, are sketched. Note that the sketch for the $SmC^*_{1/3}$ phase at 0 V illustrates the relaxed, helical state of the phase. It is thus not equivalent to the corresponding micrograph which reflects the dynamic behaviour.

Downloaded At: 17:51 25 January 2011

only the half-pitch band SmC* reflection (§ 3.1.2), which is consistent with a non-tilted helix. We will return to the issue of the SmC* phase in these materials, and how it is affected by surface action, in § 3.2.1.

The $SmC^*_{1/4}$ phase also showed a rather complex response to the applied triangular a.c. field (figure 4, upper row). When the voltage passed through zero, the conoscopic image revealed a non-tilted uniaxial macroscopic indicatrix. With 435 nm wavelength illumination, the images of the $n = 11$ and $n = 12$ homologues had bright centres with the cross being barely visible; this is a clear indication that the $SmC^*_{1/4}$ structure is optically active. However, at a wavelength of 600 nm, the optical activity had diminished such that the cross was clearly visible. In 10F1M7, finally, the cross was always clearly visible and no sign of optical activity was observed in this phase regardless of the wavelength used (the wavelengths were in this study of course limited to the visible spectrum).

With an applied field of 0.7 V μm^{-1}, the isogyres separate by a large distance perpendicular to the field direction for all three homologues. This means that the indicatrix biaxiality is high and that the helix must therefore be unwound or close to unwound. However, in contrast to what was observed in the SmC* phase, the image now stayed almost centred along the viewing direction, even though a careful look at the outer isogyres reveals that the indicatrix did in fact tilt slightly (about 1°–3°). The liquid crystal was thus still far from the fully switched, synclinic, state. It therefore seems that, in the $SmC^*_{1/4}$ phase, it is possible to unwind the helix by means of an electric field of moderate strength, inducing only a slight distortion of the equilibrium antipolar unit cell configuration. On increasing the field strength further, the conoscopic image changed drastically at a threshold field of approximately 0.9 V μm^{-1}. The macroscopic indicatrix was now clearly tilted perpendicular to the field, while it was biaxial with the optic axes in a plane *parallel* to the field. This image very much resembles that of the unwound $SmC^*_{1/3}$ image (see below) but with a larger indicatrix tilt. A possible explanation is that the threshold field corresponds to a transition from the polarization-cancelling configuration proposed in the distorted clock model to a non-cancelling structure where the director points more or less in the same direction in three out of the four layers comprising the unit cell; cf. figure 4, left and right ends of the upper section. The maximum voltage of the amplifier was insufficient to achieve the synclinic state (analogous to unwound SmC*) which must be the final state in the switching process.

In the $SmC^*_{1/3}$ phase (figure 4, lower section) the isogyres split along the direction of the applied field even at intermediate field strengths. Furthermore, the indicatrix clearly tilted perpendicular to the field. Starting out from the disturbed clock model three-layer unit cell, this may be explained by two of the three directors being distorted towards the same direction, resulting in a non-polarization-cancelling structure. Again, the magnitude

of the maximum field strength was insufficient to produce a synclinic structure. An interesting observation, common to all three homologues, is that the image at zero volts in this phase was both tilted and biaxial, and very blurred, even at a switching frequency as low as 1 Hz. First slightly *after* passing 0 V, we observed the 'relaxed' uniaxial indicatrix which was, however, tilted in this state. This hysteresis indicates that the relaxation back to the initial helical state is very slow in this phase.

In figure 4, the director configurations of the four- and three-layer unit cell phases have been drawn to conform with the conoscopy observations and also with the dielectric spectroscopy results. They imply that the mesoscopic polarization [15] is zero in $SmC^*_{1/4}$ but non-zero in $SmC^*_{1/3}$. The configurations are consistent with a distorted clock model which was also recently deduced by other methods by Johnson *et al.* [7]. However, the $SmC^*_{1/4}$ phase in the 10F1M7 compound showed no sign of optical activity and thus may have a structure compatible with the undisturbed clock model (the absence of optical activity in the clock model descriptions of $SmC^*_{1/4}$ and $SmC^*_{1/3}$ is the main objection to the model [3]). Obviously, it could very well be possible that such a four-layer period may exhibit slightly different structures in different compounds.

In the SmC^*_A phase of all homologues, only a small splitting of the isogyres perpendicular to the field direction was observed at maximum field strength. This splitting, which was much smaller than in the other tilted phases, can be attributed to an incomplete helix unwinding.

Downloaded At: 17:51 25 January 2011

3.1.2. *Transmittance measurements*

Selective reflections within the wavelength range of the spectrophotometer were easily distinguished as a sharp dip in the transmittance spectrum, occurring at a wavelength equal to the helical pitch multiplied by the average refractive index [29]. The selective reflection wavelength values thus obtained are given in figure 5. In the SmC^*_A phase, the pitch was found to become shorter with increasing length of the molecular terminal chain, and for all three homologues it decreased with increasing temperature, most conspicuously in 10F1M7. In the SmC* phase (only present in the $n=11$ and $n=12$ homologues), the pitch variation with temperature was larger and strongly non-linear. The relationship between terminal chain length and pitch was the opposite of that for the SmC^*_A case; the maximum selective reflection wavelength of 12F1M7 was slightly larger than that of 11F1M7 (460 and 445 nm, respectively).

Also for 10F1M7, we performed transmittance measurements in the temperature range between $SmC^*_{1/4}$ and SmA*—both in the relaxed state and with an electric field applied across the film—in order to verify that the phase here is really SmC^*_α and not a very short pitch

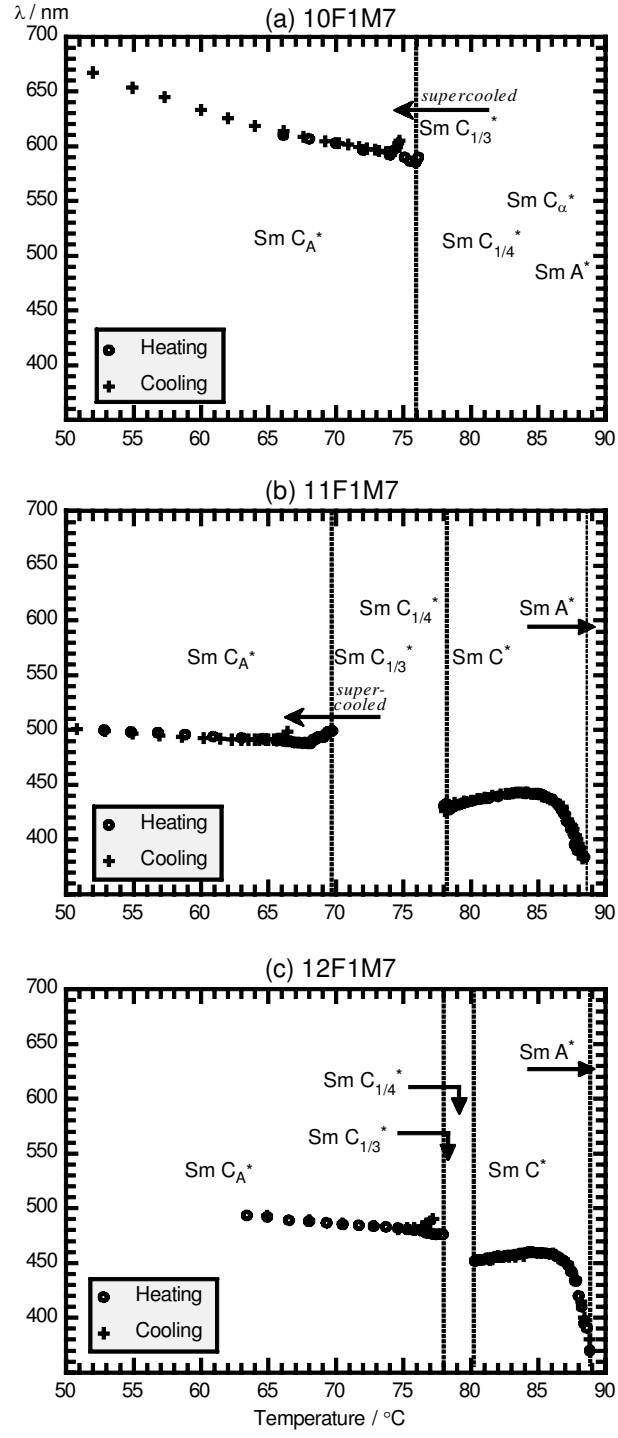

Figure 5. Selective reflection wavelength as a function of temperature for (*a*) 10F1M7, (*b*) 11F1M7 and (*c*) 12F1M7. A selective reflection wavelength of 500 nm roughly corresponds to a 300 nm helical pitch. The dashed lines indicate the approximate borders of the subphase region.

SmC* phase. However, under no circumstances could we detect a selective reflection in this phase. Had the phase been SmC*, a selective reflection would be expected at

least under application of an intermediate electric field; that is, a field strong enough to expand and distort the helix, producing a full-pitch band reflection [30], but below the threshold for complete unwinding.

In the temperature range of $SmC^*_{1/3}$ and $SmC^*_{1/4}$, no selective reflection dip was observed in any of the compounds, a result which we attribute to the long pitch in these phases, producing a selective reflection at a wavelength beyond the measuring range of our spectrophotometer. Still, in the case of 11F1M7, valuable information on the helicoidal structure in these phases was gathered from the spectra. The transmittance at 700 nm, outside the selective reflection band, was measured throughout the whole mesophase range. Within the temperature range of the long pitch subphases, a pronounced minimum in the transmittance level was observed both on heating and on cooling, cf. figure 6. We attribute this decrease (typically from 90% to 80% transmission) to a maximum in director fluctuations producing a highly scattering sample. Such fluctuations are typical of a helix inversion, and we have observed the same effect at helix inversions within the SmC* or SmC^*_A phases of other compounds [31]. The fluctuations could also be the result of a phase transition, and indeed each phase transition in the studied temperature range can be correlated with a small, but clearly visible transmittance dip in figure 6. As only one dip is seen in the temperature range between SmC^*_A and SmC*, we believe that the $SmC^*_{1/3}$–$SmC^*_{1/4}$ transition and the helix inversion actually take place simultaneously. A helix inversion within this subphase temperature range is to be expected, as the SmC* and SmC^*_A helices have opposite handedness, as confirmed by observing the films in reflection through circular polarizers.

In all three homologues, the measured pitch values at each temperature were similar on heating and on cooling. However, while the SmC*–$SmC^*_{1/4}$ transition temperature was virtually independent of temperature scan direction, the temperature at which the SmC^*_A selective reflection appeared on cooling was between 1 K (12F1M7) and 3.5 K (11F1M7) lower than the temperature at which it disappeared on heating. Such strong supercooling, also observed for the $SmC^*_{1/3}$–$SmC^*_{1/4}$ transition in figure 6, is a clear sign that the phase transition is of the first order. We will pursue the discussion on the nature of the phase transitions later in the paper.

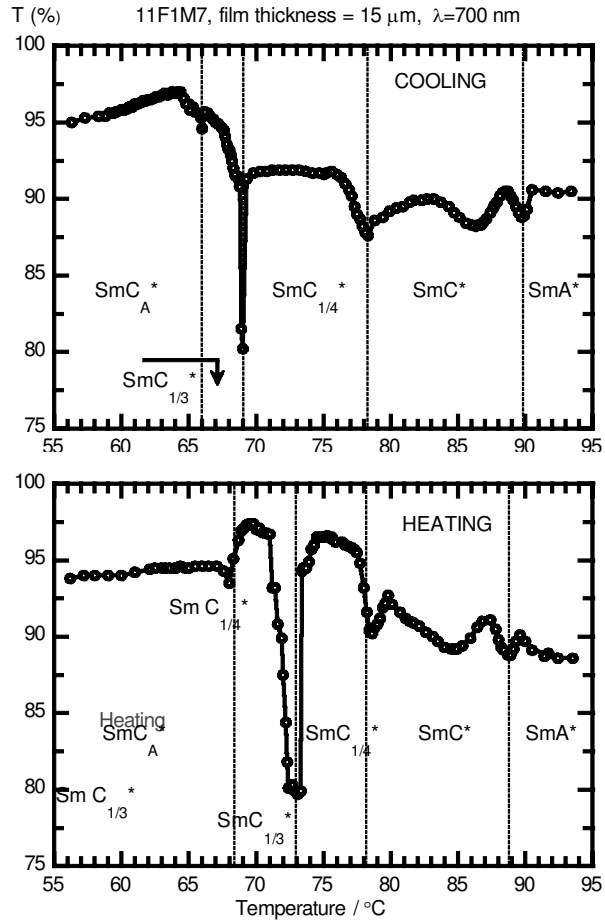

Figure 6. Transmittance level far from the wavelength of selective reflection as a function of temperature for 11F1M7. The dip-like minima in transmittance, occurring at the temperatures indicated by the dashed lines, presumably correspond to increased levels of scattering, which may be expected at a phase transition. The very prominent dip within the $SmC^*_{1/3}$/$SmC^*_{1/4}$ temperature range, in addition probably reflects the helix inversion.

3.2. *Behaviour of the compounds confined in cells*

3.2.1. *Dielectric spectroscopy*

The dielectric absorption spectra obtained at large cell gaps d ($\geqslant 30\,\mu m$) give clear evidence of the different phases present in the three homologues. In the SmC^*_A phase, the two weak modes typical for this phase [32] were detected, even though this was more difficult than in conventional samples of the same thickness. This was due to the unusually small electrode area of the wedge cells (approximately a factor of ten smaller than in standard test cells), resulting in a signal strength too low to allow modes of very low susceptibility to be easily distinguished. The transition to the $SmC^*_{1/3}$ phase was recognized by the gradual development of the prominent low frequency helix distortion ('Goldstone') mode (in the following text referred to as the HD-mode), demonstrating that the phase can have a non-zero mesoscopic polarization. This occurred at approximately 76.5, 70 and 79.5°C in 10-, 11- and 12 F1M7†, respectively, values

† The dielectric spectra of the $n = 12$ homologue are omitted for space-saving reasons. Qualitatively, this compound behaves much like 11F1M7.

Downloaded At: 17:51 25 January 2011

which agree well with the results of the transmittance measurements on the free-standing films.

In contrast to the case of the SmC* HD-mode, the susceptibility of this mode in $SmC^*_{1/3}$ was found to vary much throughout the phase temperature range in all three homologues. As the susceptibility of the HD-mode is proportional to the pitch and mesoscopic polarization squared [33], this behaviour suggests that either one of these parameters, or both, change drastically with temperature within the $SmC^*_{1/3}$ phase‡. If the variation is in the mesoscopic polarization, this implies that the three-layer unit cell changes configuration continuously within the phase. Close to the borders of the phase temperature range, where the susceptibility is very low, it would correspond to the polarization-cancelling undistorted clock model, i.e. the unit cell is characterized by a constant phase angle difference $\Delta\phi$ between two consecutive layers. In the middle of the phase, where the susceptibility of the mode was found to be large, the structure would be better described by a distorted clock model, producing a non-zero mesoscopic polarization. The other explanation, a strongly temperature-dependent pitch, is supported by the response of 10F1M7 at a 10 μm cell gap on heating (figure 7, middle). Directly after the SmC^*_A–$SmC^*_{1/3}$ transition, the absorption increased in a manner similar to the $d = 46$ μm case. Long before reaching the maximum level observed in the thick sample, however, it now stabilized and then exhibited a plateau for the rest of the phase temperature range, 77–79°C. This suggests that the 10 μm sample very soon became 'thin' in comparison with a rapidly diverging pitch on heating from SmC^*_A, and thus the helix was expelled. The absorption seen throughout the remainder of the phase was then at this cell gap no longer related to a helix distortion, but to phase angle fluctuations in the surface-stabilized structure, not representative for the bulk $SmC^*_{1/3}$ phase. As the central absorption frequency of the $SmC^*_{1/3}$ HD-mode is in the order of Hz or lower, and hence outside the measuring range of our equipment, we cannot presently draw any conclusions regarding the temperature dependence of the relaxation time of the mode. A low frequency study of the mode could probably resolve the question of which parameter varies most within the phase, since a pitch variation will be reflected in the absorption frequency, while a polarization variation will not [34].

The transition between $SmC^*_{1/3}$ and $SmC^*_{1/4}$, a phase exhibiting no strong absorptions, and hence consistent with a zero mesoscopic polarization model, was in all three homologues difficult to locate distinctly (cf. the example of 11F1M7 in figure 8, upper row). The diffuse transition implies a large degree of coexistence between the two subphases. Furthermore, the transitions to, from and between these subphases occurred with supercooling

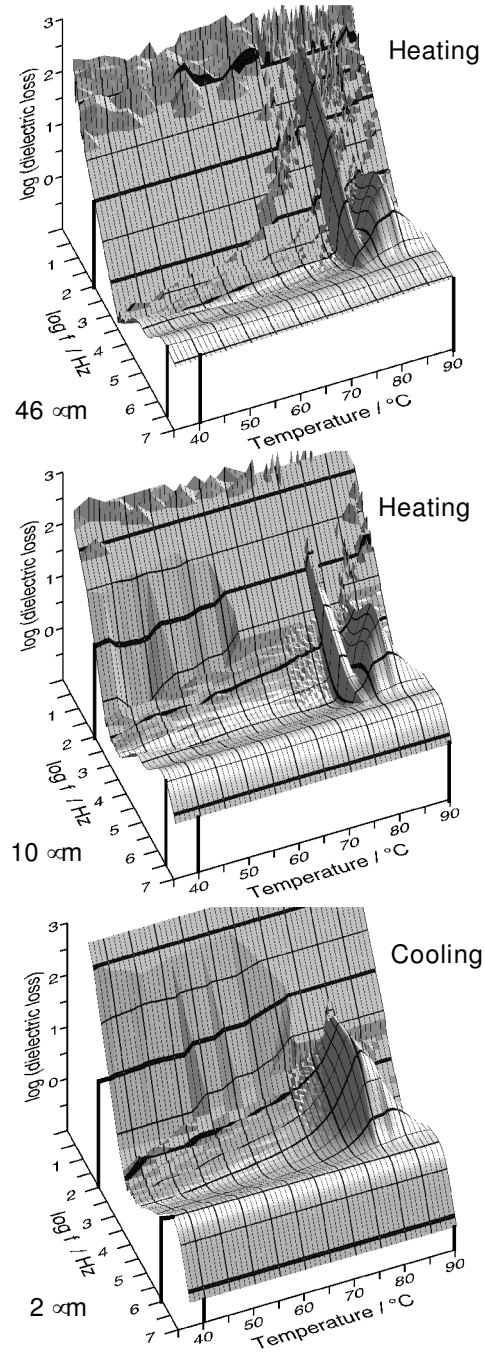

Figure 7. Dielectric loss spectra for three different thicknesses in the wedge cell with 10F1M7. The first two spectra are obtained on heating, the third on cooling. As a guide to the eye, vertical lines have been drawn connecting the values on the axes to the grid of the spectrum.

‡The tilt angle and the elastic constant also enter the expression for the HD-mode susceptibility, but it is less likely that these parameters exhibit large variations within the phase temperature range.

Downloaded At: 17:51 25 January 2011

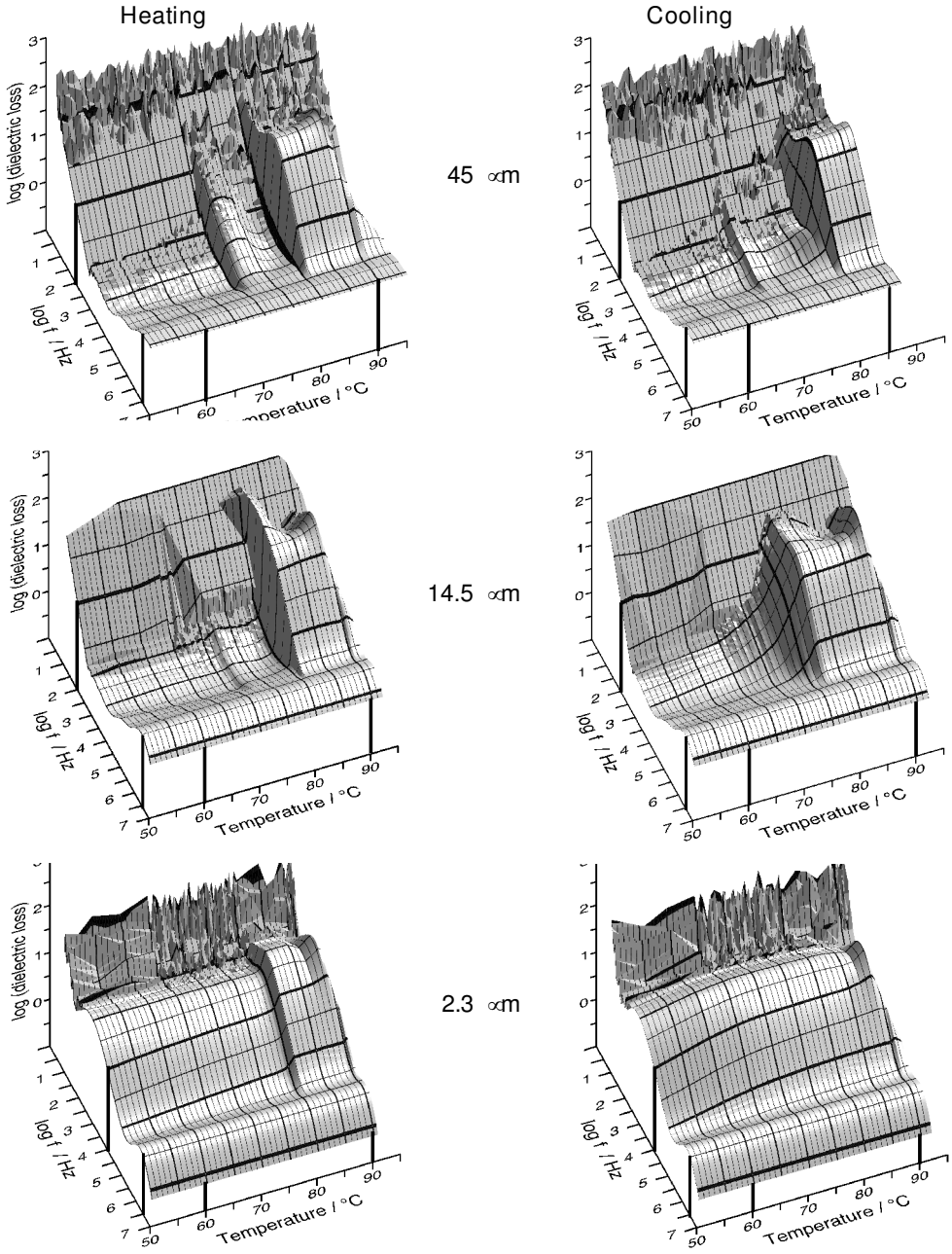

Figure 8. Dielectric loss spectra on heating and on cooling for three different thicknesses in the wedge cell with 11F1M7. The behaviour of 12F1M7 is similar but the subphase temperature range is much larger in 11F1M7, making it easier to distinguish the typical response of these phases. As a guide to the eye, vertical lines have been drawn connecting the values on the axes to the grid of the spectrum. The cooling measurement at 45 μm cell gap was started at 87°C, but for comparative reasons the data are plotted with the same scale as the other spectra.

in all three homologues, while the SmA*–SmC* or SmA*–SmC^*_α transitions occurred at the same temperature regardless of the direction of temperature change. Except for the case of the SmC*–$SmC^*_{1/4}$ transition, the same supercooling effects were also clearly observed in the spectrophotometric studies on free-standing films. This proves that the phenomena, at least in the cases of the $SmC^*_{1/4}$–$SmC^*_{1/3}$ and $SmC^*_{1/3}$–SmC^*_A transitions, were not due to surface pinning effects. The supercooling and phase coexistence are both indications that all internal transitions within the chiral smectic C phase family are first order, while the transition between orthogonal and tilted smectics is mainly second order.

In the SmC* phase at large cell gaps, both 11- and 12 F1M7 showed a response typical of the phase, characterized by a stable high susceptibility HD-mode with a

Downloaded At: 17:51 25 January 2011

central absorption frequency of approximately 5 kHz. In contrast, the large cell gap response of 10F1M7 between the $SmC^*_{1/4}$ and SmA* phases was dominated by the soft mode, peaking at the low temperature boundary of SmA*. Such a behaviour is to be expected in the SmC^*_α phase which, due to the small tilt and extremely short pitch, should only exhibit a very weak HD-mode.

Two major observations were common to all three homologues when decreasing the cell gap, but the effects were most important in the two homologues exhibiting the synclinic SmC* phase (see left sequence of figure 8). First, the development of the subphases was clearly affected. Both from dielectric and from textural studies it seemed that the $SmC^*_{1/3}$ phase was completely suppressed in thin cells, on cooling as well as on heating. We would like to stress that the surface influence from cells which are conventionally regarded as being rather thick was enough to alter the dielectric spectrum completely. For instance, for 11F1M7 at $d = 14.5\,\mu m$ the $SmC^*_{1/3}$ HD-mode had almost disappeared (figure 8, middle row). In thinner cells the mode was completely absent and, moreover, the texture revealed no sign of the phase appearing. Due to its very weak dielectric response, it was more difficult to draw any clear cut conclusions regarding the existence of the $SmC^*_{1/4}$ phase. It is impossible to distinguish it from a superheated SmC^*_A, and a coexisting supercooled SmC* component would completely cover any $SmC^*_{1/4}$ response.

The other striking effect of cell gap reduction was the appearance of a surface-induced mode, not present in the $d \sim 45\,\mu m$ measurements. Two different types appeared depending on whether or not the compound exhibited a SmC* phase. In 11- and 12 F1M7 the frequency of the mode is solely determined by the cell geometry; the lower the cell gap, the higher the absorption frequency. This behaviour is reminiscent of the surface-induced director-twist fluctuation described by Novotna *et al.* [35] (referred to by them as 'thickness mode') for the SmC* phase of FLCs, as well as of the surface layer mode proposed by Bourny *et al.* [9] for the SmC* phase of AFLCs. In both cases, the absorption frequency should follow an inverse square relationship with the cell gap. Also in our case it was possible to fit such a function quite well to the data; see figure 9. Similar to the reports of Bourny *et al.*, the mode in our case developed most easily close to the low temperature border of the SmC* phase, and on heating it was in fact present just after the $SmC^*_{1/4}$–SmC* transition even at $d \sim 45\,\mu m$. Between $d = 10$ and $d = 15\,\mu m$, it dominated much of the SmC* spectrum in all measurements. In cooling runs at these cell gaps, it was also obvious that the mode (and thus the structure giving rise to it), was heavily supercooled, with the effect of completely covering any subphase response. At $d = 2\,\mu m$, the surface-induced mode in 11F1M7 did not disappear at all, but only slightly diminished in intensity around 65°C on cooling (cf. figure 8, lower row). On reheating, the mode existed unchanged throughout the whole SmC^*_A bulk temperature range, as well as that of $SmC^*_{1/3}$ and $SmC^*_{1/4}$, but at the transition to the SmC* phase a distinct step in the absorption level was detected. We thus conclude that the mode can exist also in the SmC^*_A phase, or perhaps in a mixture of SmC* and SmC^*_A, even though the temperature range of such coexistence would then be quite remarkable.

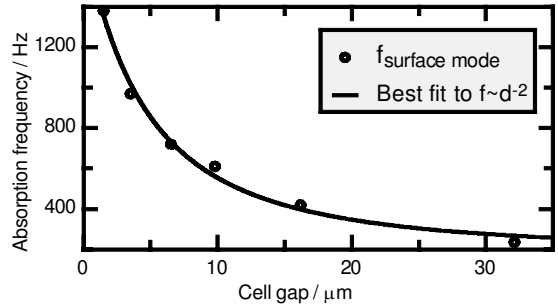

Figure 9. The absorption frequency of the surface-induced mode as a function of cell gap for 12F1M7 and the best fit to the $f \sim d^{-2}$ relationship proposed for such a mode by Novotna *et al.* [35] and Bourny *et al.* [9].

Panarin *et al.* [16, 22] have observed the same mode in 12F1M7 as well as in other AFLC compounds, not discussed here. They interpret its appearance as a sign of a phase transition from the normal SmC* to a phase they denote 'FiLC', coinciding in temperature with the observations of the blurry switching image during conoscopy studies (see § 3.1.1). As they find the absorption frequency of the new mode to be the same as that of the HD-mode in $SmC^*_{1/3}$, and as the normal SmC* HD-mode is clearly still present, they suggest that the new phase in fact is a coexistence of ferri- and ferroelectric structures. However, they fail to recognize the strong cell gap dependence of the absorption frequency of the new mode. This dependence clearly shows that the mode is connected to a surface-induced structure and cannot thus be a feature of the liquid crystal phase in itself. Furthermore, bearing in mind how the $SmC^*_{1/3}$ (the only well established phase which could possibly be regarded as ferrielectric) response is easily quenched even by moderate surface action, the explanation of Panarin *et al.* would imply a vanishing of the mode, rather than the increased importance observed here, on decreasing the cell gap (see figure 8). The dependence on cell gap of the temperature at which the new mode appears, in addition to the fact that the normal SmC* HD-mode seems little disturbed by its appearance, also contradicts the idea that a change of thermodynamic phase is involved.

Downloaded At: 17:51 25 January 2011

On the other hand, it is possible that the SmC* phase exhibited by 11- and 12 F1M7, and probably by any antiferroelectric liquid crystal exhibiting this phase, is inherently different from the SmC* phases of standard FLC materials. The tendency towards antipolar, anticlinic order in AFLCs may disturb the synclinic, synpolar order of the SmC* phase, probably most severely close to the low temperature border of the phase. These ideas, compatible with the reasoning of Bourny *et al.* [9] and Pavel *et al.* [10], will be presented in detail separately [12].

In both the director-twist model of Novotna *et al.* and the surface-layer mode model of Bourny *et al.*, the mechanism behind the absorption is a fluctuation in a surface-induced inhomogeneous polarization configuration within each layer. Also in our case, such a fluctuation is most certainly the underlying mechanism, but it is not yet clear which of the models, if any, correctly describes the behaviour. Further studies are being performed in order to elucidate the true nature of the absorption and the results will be presented elsewhere [12]. What can clearly be seen at the present stage, is that the mode can appear in any phase within the chiral smectic C family.

In order to investigate the behaviour of the surface-induced mode in a standard measurement cell during switching studies, a run was also performed on a uniform 4 μm measurement cell (both substrates coated with polyimide, antiparallel buffing) with 11F1M7, where impedance scans were taken both with an applied bias d.c. field (above the threshold for switching to the synclinic state) and directly after releasing the field. While all modes except the soft mode were fully suppressed in the d.c. ON spectrum, the spectrum obtained after removing the bias fully resembled that of the corresponding d.c.-free run on the wedge cell, including the large degree of supercooling of the surface-induced mode. This means that one must consider, at least in the case of thin cells, the possibility of a non-uniform polarization configuration being present in any chiral smectic C phase. As this is always connected to a non-uniform director, and hence optic axis, structure, such a state may also severely affect the results of other investigation techniques, e.g. electro-optical studies. There is thus a call for care when analysing experimental results on the various chiral smectic C phases obtained in samples thinner than, say, 25 μm, in particular if these are from observations made on cooling.

The homologue without a normal synclinic SmC* phase, 10F1M7, also developed a surface-induced, or perhaps surface-amplified, absorption when the cell gap was reduced, but this was of a slightly different nature. No 'typical' HD-mode was observed in the SmC^*_α phase regardless of cell gap, but there was clearly another mode active in addition to the soft mode. This mode

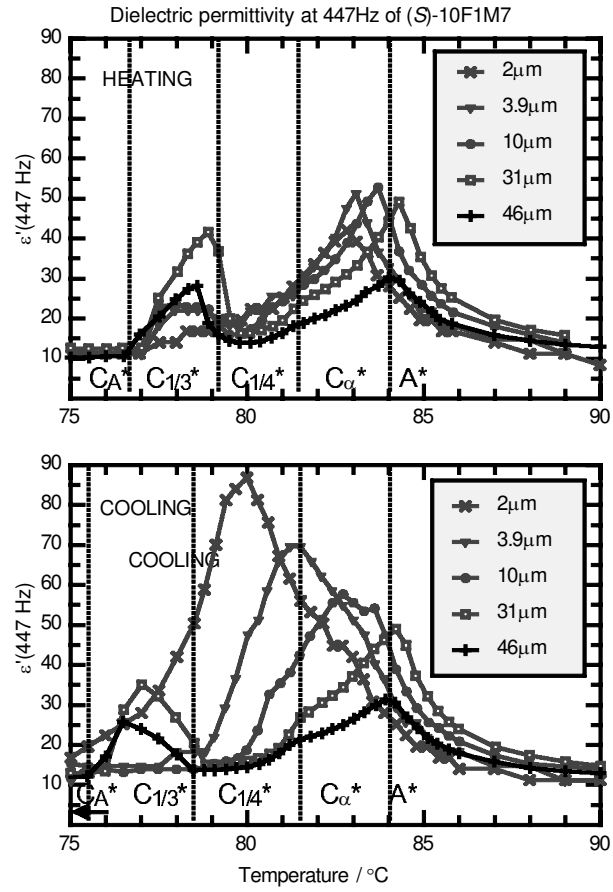

Figure 10. The real part of the dielectric permittivity at 447 Hz as a function of temperature for 10F1M7 in samples of varying thickness. The phase transition temperatures indicated in the figure are based on the 46 μm measurements, drawn with black lines. On reducing the cell gap, the $SmC^*_{1/3}$ HD-mode is first enhanced at $d = 31$ μm, but then suppressed below the $d = 46$ μm response at lower cell gaps. Note also how the response on cooling becomes dominated by a surface-induced mode when reducing the cell gap.

was barely visible in the $d = 46$ μm measurement, but it grew stronger with decreasing value of d (cf. figures 7 and 10). The intensity was very temperature dependent, with a maximum some degrees below the SmA*–SmC^*_α transition. At $d < 10$ μm this maximum absorption intensity was much higher than that of the soft mode, cf. figure 10. One may therefore get the erroneous impression that the soft mode maximum, and hence the actual phase transition, is shifted downwards in temperature when decreasing the cell gap§. A similar SmC^*_α absorption has been observed by Simeão *et al.* [36] where it is said to

§Some supercooling of the SmA*–SmC^*_α transition probably *is* induced by reducing the cell gap, as is suggested by the electro-optical studies to be discussed. This effect is, however, not at all as large as the dielectric spectra may suggest.

Downloaded At: 17:51 25 January 2011

be 'triggered' by the soft mode. It is unclear to us what is meant by this, but seeing how the mode increases greatly in magnitude when reducing the cell gap, we find it most probable that the mode reflects fluctuations in a surface-induced structure. This could either be a structure similar to that found in the other homologues, or it could be a coexistence of bulk SmC^*_α and a SmC*-like structure close to the surfaces, giving rise to a measurable HD-mode, supported by the synclinic/synpolar surface-ordering [18]. The first alternative is, however, not really compatible with the observed strong temperature dependence of the absorption frequency and intensity of the mode.

A third observation related to the reduction of d was that all supercooling effects grew stronger in thin cells, hence supporting the idea that synclinic structures are promoted by surface influence. In particular, both surface-induced modes had a strong tendency to supercooling. Also the $SmC^*_{1/3}$–SmC^*_A transition, which for 10F1M7 was distinguished down to $d = 7\,\mu m$, was pushed downwards in temperature as the measurement cell gap was reduced.

Downloaded At: 17:51 25 January 2011

3.2.2. *Textures at large cell gap*

During all dielectric spectroscopy measurements the planar texture in a thick ($d \sim 35\,\mu m$) part of the cell was monitored to assess the possibility of directly correlating changes in texture with changes in the dielectric spectrum. Examples of the textures formed on cooling from the isotropic phase are given for 10F1M7 and 12F1M7 in figures 11 and 12, respectively. The presence or absence of the synclinic SmC* phase obviously has a large effect on the textures of the other tilted smectic phases. The 11- and 12 F1M7 homologues showed very similar texture sequences, while 10F1M7, exhibiting no synclinic SmC* phase, differed from the others in several respects, at least at $d \geqslant 35\,\mu m$.

The SmA*–SmC^*_α transition in 10F1M7 (see figure 11) did not produce any drastic changes in texture. Only a slight rippling of the backs of the focal-conics, and a weak pink colour tone distinguish SmC^*_α from SmA*. The transition to $SmC^*_{1/4}$, on the other hand, was easily spotted in spite of the paramorphotic character of all textures. First, the long pitch of this phase led to the appearance of coarse stripes (pitch lines) parallel to the layers. The second, and more surprising observation was that the dark crosses of the confocal domains, i.e. the perspectivic crossings of disclination ellipses and hyperbolae [37], separated into two halves within this phase as well as in the $SmC^*_{1/3}$ phase. A careful look at the texture images reveals that the ellipse had a particular tendency to break up. In fact, even in the SmA* phase a slight zigzag modulation of the ellipse was seen in some focal conics. The hyperbolic disclination line stayed

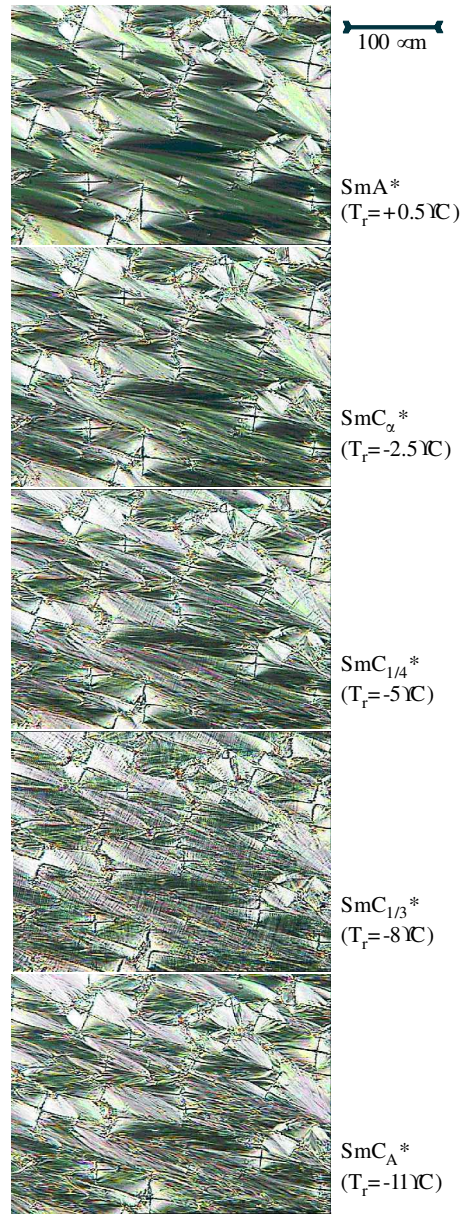

Figure 11. Textures formed on cooling from the isotropic phase of planar-aligned 10F1M7 at ~35 μm cell gap. Temperatures are given in relation to the transition from the orthogonal SmA* phase. The sample is placed between crossed polarizers, the directions of which are approximately vertical/horizontal. Note the breaking-up of the disclination lines at the centres of the focal conics, within the two subphases $SmC^*_{1/3}$ and $SmC^*_{1/4}$. The lines closest to the vertical direction are the ellipses, while the almost horizontal lines are the hyperbolae.

intact longer, but in the $SmC^*_{1/3}$ phase, which exhibited the greatest separation of the singularity lines as well as the most coarsely striped texture, this was again clearly broken. To our knowledge, this textural characteristic of the $SmC^*_{1/4}$ and $SmC^*_{1/3}$ subphases has not been reported before. At present we are uncertain about the

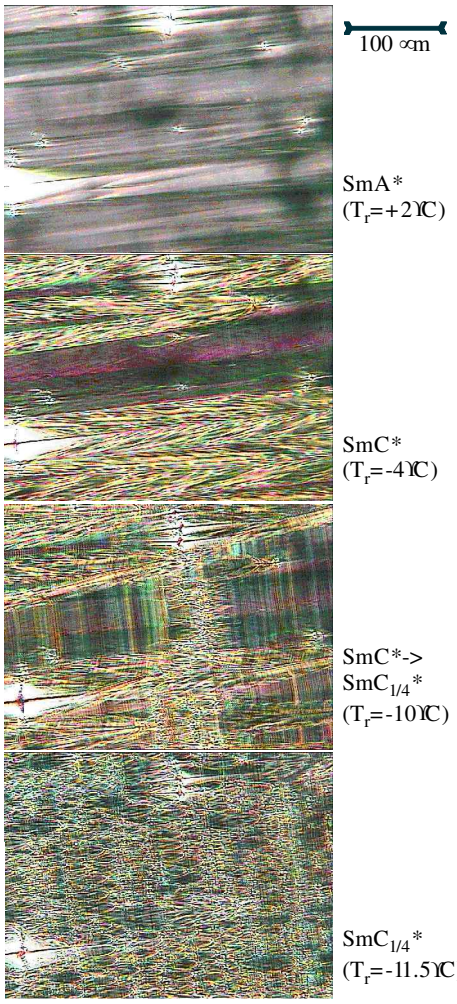

Figure 12. Textures formed on cooling from the isotropic phase of planar-aligned 12F1M7 at ~35 μm cell gap. Temperatures are given in relation to the transition from the orthogonal SmA* phase. The sample is placed between crossed polarizers, the directions of which are approximately vertical/horizontal. Note the drastic change in texture after the transition from SmC* to $SmC^*_{1/4}$.

underlying nature of this change, which we also observed in other compounds exhibiting these subphases and also in standard uniform measurement cells. On continued cooling, the onset of SmC^*_A was easily recognized by the focal-conic disclinations reforming the normal crosses (figure 11, lowest picture). In fact, the SmC^*_A texture of 10F1M7 looked very similar to that of SmC^*_α.

At the SmA*–SmC* transition that occurrs in the two other homologues, two types of fairly broad ribbons appeared, directed along the buffing direction. One type had a smooth, slightly reddish, dark texture, while the other was distinguished by a fishskin-like set of defects rendering these areas much brighter in the polarizing microscope image; see the example of 12F1M7 in figure 12. By applying an electric field over the sample such that the helix unwinding commences, hence giving rise to striping along the layers, we were able to see how the layers were directed in the two ribbon types. In the former type, the layers were perpendicular to the rubbing direction, as in SmA*, while the defect-rich ribbon type proved to contain horizontal chevrons. In general these ribbons consisted of two halves in which the layer normal was inclined at a positive angle, typically 20°–30°, in one half, and at the same angle but with negative sign, in the other.

The transition to the $SmC^*_{1/4}$ phase produced a drastic texture change, as can be seen in the two lower pictures of figure 12. At the onset of the transition, coarse stripes appeared, often with rather intense colours. At the same time, parabolic defects invaded the texture, and these grew in number at such speed that the texture had completely changed when the phase transition was completed; see lower picture of figure 12. Parabolic defects appear as a result of dilative layer strain [38]. Such strain appears at a sudden decrease in layer thickness and the sudden explosion of parabolic defects at the SmC*–$SmC^*_{1/4}$ transition in both 11- and 12 F1M7 thus indicates that this transition is connected with a discontinuous decrease in molecular tilt. To corroborate this hypothesis, a careful X-ray study should be made in the vicinity of this transition.

The transition between $SmC^*_{1/4}$ and $SmC^*_{1/3}$ produced no visible texture change in either 11F1M7 or 12F1M7. On continued cooling to SmC^*_A, the stripes gradually disappeared, but the exact temperature of the transition to this phase could not be obtained from texture studies alone.

The textural descriptions given above, and the differences between the samples, apply to rather large cell gaps. The defects generated as the temperature was lowered for 11F1M7 and 12F1M7 were actually also observed in 10F1M7, but at a much smaller cell gap (~10 μm), again indicating that a lowering of the cell gap enhances a synclinic ordering in chiral smectic C phases.

3.2.3. *Preliminary electro-optical investigations*

With the results from dielectric spectroscopy in mind, one would also of course like to perform electro-optical investigations in cells sufficiently thick for no surface-induced structures to develop. This would, however, mean utilizing cells with $d \geqslant 30$ μm and as it is not easy to obtain a homogeneous mono-domain alignment in such cells, we have chosen to study cells with $d \leqslant 10$ μm, realizing that many of the results may be attributed to a surface-generated structure rather than to the architecture of the bulk phase under study.

In all cells the magnitude of the observed hysteresis decreased with decreasing frequency. In the $d \sim 1.4$ μm

Downloaded At: 17:51 25 January 2011

cells with 12F1M7, the switching was SmC*-like but with a smooth change in transmission ('V-shape'-like) throughout the whole mesophase range below SmA*, see figure 13, right column. In contrast, 10F1M7 (figure 14) showed a larger difference in switching behaviour between the different mesophases, even in thin cells. Comparing with the dielectric spectroscopy results, this indicates that in 12F1M7 the switching behaviour was dominated by the response of the supercooled surface-induced SmC* state even at temperatures well below the bulk temperature range of SmC*. The response of 10F1M7, which did not possess the surface-induced mode in SmC_A^* even in the thinnest part of the wedge cell, can be regarded as more representative of the bulk phase structure. This illustrates that the switching behaviour in thin cells with AFLCs exhibiting a SmC* phase, in general cannot be attributed to the bulk phase but rather to the particular geometry (or even the thermodynamic phase) which is stable under the condition of the closely spaced polar surfaces. It has previously been shown [18] that so-called 'V-shaped switching', a very attractive mode for electro-optical devices, can be related to a surface-induced, polarization-stabilized twisted structure in SmC*. As the smooth switching behaviour of 12F1M7 is only observed at very low frequencies, and is in general not hysteresis-free, it is of no interest from an applicational point of view, but it is probably the result of a similar kind of surface-generated twist.

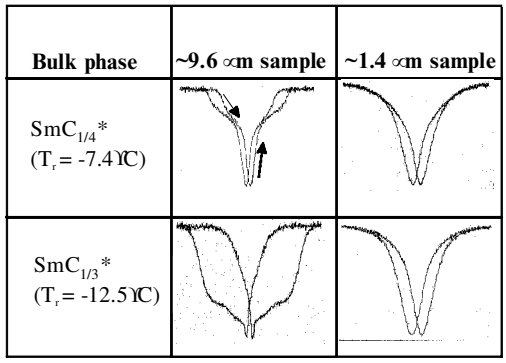

Figure 13. Electro-optical switching characteristics of ~9.6 and ~1.4 μm samples of (*S*)-12F1M7 at temperatures where the bulk material is in the $SmC^*_{1/4}$ and $SmC^*_{1/3}$ phases, respectively. Temperatures are given in relation to the transition from the orthogonal SmA* phase; the switching frequency is 0.1 Hz. While the $SmC^*_{1/4}$ and $SmC^*_{1/3}$ responses at $d \sim 9.6$ μm differ from that of SmC*, the SmC* response of the 1.4 μm sample remains far below the low temperature limit of SmC* in bulk. This indicates that phase and structure transitions are suppressed in the thin cell.

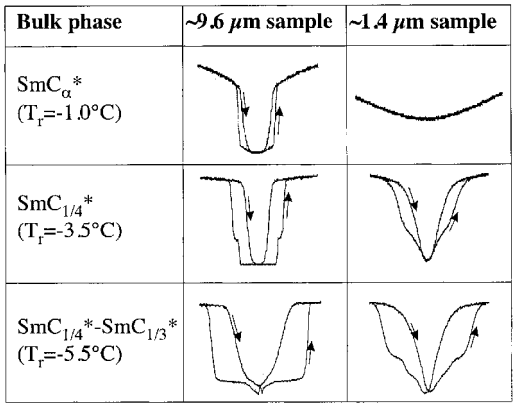

Figure 14. Electro-optical switching characteristics of ~9.6 and ~1.4 μm samples of (*S*)-10F1M7 at temperatures where the bulk material is in the SmC^*_α, $SmC^*_{1/4}$ and $SmC^*_{1/3}$ phases. Temperatures are given in relation to the transition from the orthogonal SmA* phase; the switching frequency is 0.1 Hz. Note the electroclinic-like switching in the $d \sim 1.4$ μm sample at temperatures where the bulk sample has changed from SmA* to SmC^*_α. The reduction in cell gap thus seems to induce a supercooling of the SmA* phase.

Of note is the apparent tristate switching observed in the (nominally) SmC^*_α phase of 10F1M7 in both the 9.6 μm (figure 14, upper row) and 3.9 μm thick cells. This behaviour is consistent with previous observations on the SmC^*_α phase [39, 40]. Interestingly, in the same temperature range, the thinnest cell (1.4 μm) exhibited only a weak electroclinic response (figure 14, upper row, right column), suggesting that the surface action induced a supercooling of the SmA* phase.

The electro-optical response in the temperature range where the bulk sample is in the $SmC^*_{1/3}$ or $SmC^*_{1/4}$ phase, is characterized by 'steps' in the transmission at a voltage below complete switching to the ferroelectric state. This is most clearly seen in the 0.1 Hz curves obtained with ~10 μm thick samples. While this behaviour was easily suppressed by decreasing the cell gap for 12F1M7, some apparent subphase behaviour appeared to be preserved in the thinnest cell of 10F1M7. As this material does not possess a SmC* phase it may be regarded as a more strongly anticlinic (or weaker synclinic) material than the other homologues. For this reason the $SmC^*_{1/3}$ and $SmC^*_{1/4}$ phases may not be entirely suppressed by the increased synpolar/synclinic surface interaction of the thin cell, as they seem to be in 12F1M7.

4. Conclusions

The investigated compounds all exhibit SmC^*_A, $SmC^*_{1/3}$, $SmC^*_{1/4}$ and SmA* phases in the bulk. 10F1M7 exhibits a SmC^*_α phase between the latter two phases, while the corresponding phase in the other homologues is SmC*.

Downloaded At: 17:51 25 January 2011

Supercooling and phase coexistence tendencies are often observed at transitions between two phases of the chiral smectic C family, both in cells and in free-standing films. This suggests that all such transitions are first order. The effects in the case of cells are enhanced by reducing the cell gap.

Optical spectroscopy measurements at wavelengths outside the selective reflection band reveal a decrease in transmittance (probably an effect of an increased scattering) in the vicinity of phase transitions and/or helix inversions. The SmC^*_α phase may be identified using conoscopy through the 90° reorientation of the biaxial indicatrix which occurs during switching in this phase. We suggest that the biaxial state observed at intermediate field is a result of a combination of weak helix unwinding and a large electroclinic change in tilt angle. The $SmC^*_{1/4}$ phase of 11- and 12 F1M7 is optically active, although the observation depends on the wavelength used. 10F1M7 never exhibits an observable optical activity in this phase, and this compound may thus be an AFLC where the $SmC^*_{1/4}$ phase is compatible with the undistorted clock model. During switching, both $SmC^*_{1/4}$ and $SmC^*_{1/3}$ reach similar states just below the threshold for achieving the fully switched synclinic state, but $SmC^*_{1/4}$ exhibits an intermediate non-helical, virtually untilted, state where the biaxiality is perpendicular to the applied field. $SmC^*_{1/3}$ exhibits a much slower relaxation back to the helical zero-field state than $SmC^*_{1/4}$. In studies of the planar textures, these two phases are in 10F1M7 distinguished by a peculiar splitting of the focal-conic cross. In the other homologues, and in thin cells of 10F1M7, the transition to $SmC^*_{1/4}$ on cooling is coupled to the sudden appearance of a large number of parabolic defects. This implies a discontinuous change in tilt angle at this transition.

The results from dielectric spectroscopy show that the $SmC^*_{1/3}$ phase has a non-zero mesoscopic polarization, whereas the mesoscopic polarization is zero in $SmC^*_{1/4}$. These results are corroborated by the conoscopy studies. Dielectric spectroscopy and electro-optical investigations provide evidence that the director structure in cells thinner than ~25 μm may be more dictated by the surface conditions than the bulk phase. The dielectric spectra of the $n = 11$ and $n = 12$ homologues, both exhibiting a synclinic SmC* phase, develop a strong surface-induced mode even at relatively large cell gaps. This mode has a high tendency to supercooling and can dominate the response of the sample irrespective of which bulk phase is stable at the particular temperature. 10F1M7 also exhibits a surface-enhanced mode, but this is much less predominant and its characteristics change with temperature.

We are grateful to Dr R. A. Lewis for providing a sample of (*S*)-12F1M7 and to Dr P. Rudquist for valuable discussions. Financial support from the European ORCHIS network, the Swedish Foundation for Strategic Research and the Royal Physiographic Society (Lund, Sweden) is gratefully acknowledged.

Downloaded At: 17:51 25 January 2011

References

[1] Galerne, Y., and Liebert, L., 1989, FLC'89 conference, 27–30 June, Göteborg, Sweden, O27; Takezoe, H., Chandani, A. D. L., Lee, J., Gorecka, E., Ouchi, Y., Fukuda, A., Terashima, K., Furukawa, K., and Kishi, A., 1989, FLC'89 conference, 27–30 June, Göteborg, Sweden, O26.

[2] See for instance Takezoe, H., Lee, J., Ouchi, Y., and Fukuda, A., 1991, *Mol. Cryst. liq. Cryst.*, **202,** 85; Okabe, N., Suzuki, Y., Kawamura, I., Isozaki, T., Takezoe, H., and Fukuda, A., 1992, *Jpn. J. appl. Phys.*, **31,** L793; Skarabot, M., Cepic, M., Zeks, B., Blinc, R., Heppke, G., Kityk, A. V., and Musevic, I., 1998, *Phys. Rev. E*, **58,** 575.

[3] Akizuki, T., Miyachi, K., Takanishi, Y., Ishikawa, K., Takezoe, H., and Fukuda, A., 1999, *Jpn. J. appl. Phys.*, **38,** 4832.

[4] Mach, P., Pindak, R., Levelut, A. M., Barois, P., Nguyen, H. T., Baltes, H., Hird, M., Toyne, K., Seed, A., Goodby, J. W., Huang, C. C., and Furenlid, L., 1999, *Phys. Rev. E*, **60,** 6793.

[5] Fukuda, A., Takanishi, Y., Isozaki, T., Ishikawa, K., and Takezoe, H., 1994, *J. mater. Chem.*, **4,** 997.

[6] Zeks, B., and Cepic, M., 1998, *Proc. SPIE*, **3318**, p. 68.

[7] Johnson, P. M., Olson, D. A., Pankratz, S., Nguyen, H. T., Goodby, J. W., Hird, M., and Huang, C. C., 2000, *Phys. Rev. Lett.*, **84,** 4870.

[8] Musevic, I., 1999, *Optics and Dynamics of Antiferroelectric Liquid Crystals*, presented at a workshop on dielectric spectroscopy, 20 December, Dublin, Ireland (Organizer: Vij, J.).

[9] Bourny, V., Pavel, J., Gisse, P., and Nguyen, H. T., 2000, *Ferroelectrics*, **241,** 247.

[10] Pavel, J., Gisse, P., Nguyen, H. T., and Martinot-Lagarde, Ph., 1995, *J. de Physique II*, **5,** 355.

[11] Skarabot, M., Kocevar, K., Blinc, R., Heppke, G., and Musevic, I., 1999, *Phys. Rev. E*, **59,** R1323.

[12] Lagerwall, J. P. F., Rudquist, P., and Lagerwall, S. T., presented at FLC 2001, Washington DC, USA, submitted to *Ferroelectrics*.

[13] Pociecha, D., Szydlowska, J., Glogarova, M., and Gorecka, E., 1999, *Dielectric properties of smectic C* phase with helix twist inversion*, Abstract for the FLC'99 conference, 29 August–3 September, Darmstadt, Germany.

[14] Lagerwall, J. P. F., 2000, Licentiate thesis, Chalmers University of Technology, Göteborg, Sweden.

[15] Lagerwall, S. T., 1999, *Ferroelectric and Antiferroelectric Liquid Crystals* (Weinheim: Wiley-VCH).

[16] Panarin, Yu. P., Kalinovskaya, O., Vij, J. K., and Goodby, J. W., 1997. *Phys. Rev. E*, **55,** 4345.

[17] Cepic, M., Heppke, G., Hollidt, J. M., Lötzsch, D., and Zeks, B., 1993, *Ferroelectrics*, **147,** 159.

[18] Rudquist, P., Lagerwall, J. P. F., Buivydas, M., Gouda, F., Lagerwall, S. T., Clark, N. A., Maclennan, J. E., Shao, R. F., Coleman, D., Bardon, S., Bellini, T., Link, D. R., Natale, G., Glaser, M. A., Walba, D. M., Wand, M. D., and Chen, X. H., 1999, *J. mater. Chem.*, **9,** 1257.

[19] Moritake, H., Shigeno, N., Ozaki, M., and Yoshino, K., 1993, *Liq. Cryst*., **14,** 1283.
[20] Jägemalm, P., Lagerwall, J. P. F., Dahlgren, A., Komitov, L., Matharu, A., Grover, C., Gouda, F., and Kutub, A., 1999, *Ferroelectrics*, **244,** 447.
[21] Baylis, L. J., Gleeson, H. F., Seed, A. J., Styring, P. J., Hird, M., and Goodby, J. W., 1999. *Mol. Cryst. liq. Cryst*., **328,** 13.
[22] Panarin, Yu, P., Xu, H., MacLughadha, S. T., Vij, J. K., Seed, A. J., Hird, M., and Goodby, J. W., 1995, *J. Phys: Condens. Matter*, **7,** L351.
[23] Shtykov, N. M., Vij, J. K., Lewis, R. A., Hird, M., and Goodby, J., 2000, *Phys. Rev. E*, **62,** 2279.
[24] Panarin, Yu. P., Kalinovskaya, O., Vij, J. K., Parghi, D. D., Hird, M., and Goodby, J. W., 2000, *Ferroelectrics*, **244,** 183.
[25] Parghi, D. D., Kelly, S. M., and Goodby, J. W., 1999, *Mol. Cryst. liq. Cryst*., **332,** 313.
[26] Nishiyama, I., Chin, E., and Goodby, J. W., 1993, *J. mater. Chem*., **3,** 191.
[27] See for instance Gorecka, E., Chandani, A. D. L., Ouchi, Y., Takezoe, H., and Fukuda, A., 1990, *Jpn. J. appl. Phys*., **29,** 131; Isozaki, T., Fujikawa, T., Takezoe, H., and Fukuda, A., 1993, *Phys. Rev. B*, **48,** 13 439; Hatano, J., Hanakai, Y., Furue, H., Uehara, H., Saito, H., and Murashiro, K., 1994, *Jpn. J. appl. Phys*., **33,** 5498; Roy, A., and Madhusudana,N. V., 1998, *Europhys. Lett*., **41,** 501.
[28] See for instance Jägemalm, P., 1999, PhD thesis, Chalmers University of Technology, Göteborg, Sweden.
[29] Belyakov, V. A., and Dmitrenko, V. E., 1989, *Optics of Chiral Liquid Crystals*, Soviet Scientific Reviews A 13 (Moscow).
[30] Dahlgren, A., Buivydas, M., Gouda, F., Komitov, L., and Lagerwall, S. T., 1998, *Liq. Cryst*., **25,** 553.
[31] Gouda, F., and Lagerwall, J. P. F. (to be published).
[32] Hiraoka, K., Takezoe, H. and Fukuda, A., 1993, *Ferroelectrics*, **147,** 13.
[33] Levstik, A., Carlsson, T., Filipic, C., Levstik, I., and Zeks, B., 1987, *Phys. Rev. A*, **35,** 3527.
[34] Gouda, F., 1992, PhD thesis, Chalmers University of Technology, Göteborg, Sweden.
[35] Novotna, V., Glogarova, M., Bubnov, A., and Sverenyak, H., 1997, *Liq. Cryst*., **23,** 511.
[36] Simeão Carvalho, P., Chaves, M. R., Destrade, C., Nguyen, H. T., and Glogarova, M., 1996, *Liq. Cryst*., **21,** 31.
[37] Demus, D., and Richter, L., 1980, *Textures of Liquid Crystals* (Leipzig: VEB Deutscher Verlag für Grundstoffindustrie).
[38] Rosenblatt, C., Pindak, R., Clark, N. A., and Meyer, R. B., 1977, *J. Phys. (Paris)*, **38,** 1105.
[39] Hou, J., Schadt, M., Giesselmann, F., and Zugenmaier, P., 1997, *Liq. Cryst*., **22,** 401.
[40] Takanishi, Y., Hiraoka, K., Agrawal, V. K., Takezoe, H., Fukuda, A., and Matsushita, M., 1991, *Jpn. J. appl. Phys*., **30,** 2023.

Downloaded At: 17:51 25 January 2011